94st Annual Meeting of the Eastern Society of the Seismological Society of America

October 23rd-25th, 2022
University of South Florida
Tampa, FL

Acknowledgements

Many people contributed to the success of the ES-SSA 2022 meeting, and we would like to thank them:

Banquet Guest Speaker: Dr. Mark Rains (Chief Science Officer of the State of Florida)

Web logistics: Nan Broadbent

Student Grant and Best Student Presentation coordination: Zhigang Peng

Meeting preparation support: Zhigang Peng, Steven Jaume

Jesuit Seismological Society Award Committee

Many thanks to the session chairs!

Stephen McNutt and Jochen Braunmiller
Meeting Co-Chairs

Many thanks to our sponsors!

General Information

Welcome to the University of South Florida!

The 94th Annual Meeting of the Eastern Section of the Seismological Society of America is hosted by the University of South Florida in Tampa, Florida. The meeting will take place on 23-25 October 2022.

A **field trip** to **Karst Features in the Tampa Bay region** is on **Sunday 23 October**. Participants registered for the field trip will meet at 8:45 AM in the lobby of the Embassy Suites hotel. The field trip leaves at 9 AM. Lunch will be provided. We will return to the Embassy Suites hotel around 4:30-5:00 PM.

A **reception** will start off the meeting on the evening of **Sunday 23 October**. The reception is in the bar area of the **Embassy Suites** hotel from **6-8 PM** and we will have a cash bar.

The **Executive Committee of the ES-SSA** will meet on **Sunday 23 October at 8 pm** at the **Embassy Suites** hotel. Location TBD.

The **venue for the formal presentations is the Marshall Student Center** (MSC) located in center of the USF campus (see map). Meeting rooms are on the second floor of the MSC (see floor plan). Presentations will be on **Monday 24 October and Tuesday 25 October** and sessions will run from **8 AM to about 5 PM** (see meeting schedule below for details). Registration will open at 7:30 AM on each day.

The **Banquet and Jesuit Society Award's Dinner** will be on **Monday evening at 7-9 PM** in the **Embassy Suites** hotel Salon A,B,C preceded by a reception (6-7 PM). The Banquet Presentation will be given by Dr. Mark Rains (Chief Science Officer of the State of Florida).

This is a **hybrid meeting** with in-person and online attendees. Presentations (oral and poster) are in-person. We provide a live stream of oral presentations and online access to poster presentations for online attendees.

Presentation Information:

Speakers: Oral presentations will be 20 minutes long including questions. Equipment for PowerPoint presentations will be available. Please find out from the program when your presentation is and make sure to load your presentation on the meeting computer well in advance of your presentation. Please bring a USB stick with your PowerPoint presentation and upload BEFORE your session. The meeting is hybrid, and we will use MSTeams to stream oral presentations. We are not recording the presentations.

Posters: Poster presentations will be up during the entire meeting, and we have dedicated time slots for the posters. Poster areas are approximately X ft wide and Y ft high (**TBD**) and thumb tacks will be available. Please be near your poster during the Monday and Tuesday poster sessions. All posters have to be submitted to the meeting organizers in pdf format (see below) and will be made available to attendees during the meeting and up to about 1 month after the meeting.

Information for **Session Chairs**: A microphone will be at the lectern. Each oral presentation, including questions and change-over time is twenty minutes long.

Meeting Website:
https://www.seismosoc.org/inside-eastern-section/annual-meeting/

SRL Abstracts:
Abstracts for meetings of the Eastern Section of the SSA will be published electronically.

Travel information to and from the Tampa International Airport (TPA):
The Embassy Suites, Holiday Inn Express, and La Quinta hotels are adjacent to each other and about 18 miles from Tampa International. Taxis, Uber and/or Lyft are the most convenient form of transportation to the hotels and to the campus.

The Marshall Student Center (MSC) is about 0.75 miles (by foot) and 1.8 miles (car) from the Embassy Suites hotel (see map). Visitor parking at the MSC can be purchased at pay stations in the 3B parking lot (visitor parking permitted in "D" parking lots). The license plate is your permit and the receipt may be used as bus pass for the USF Transit System. Day passes are valid for a calendar day (not 24-hrs).

Contacts:
Steve McNutt, USF, smcnutt@usf.edu
Jochen Braunmiller, USF, jbraunmiller@usf.edu

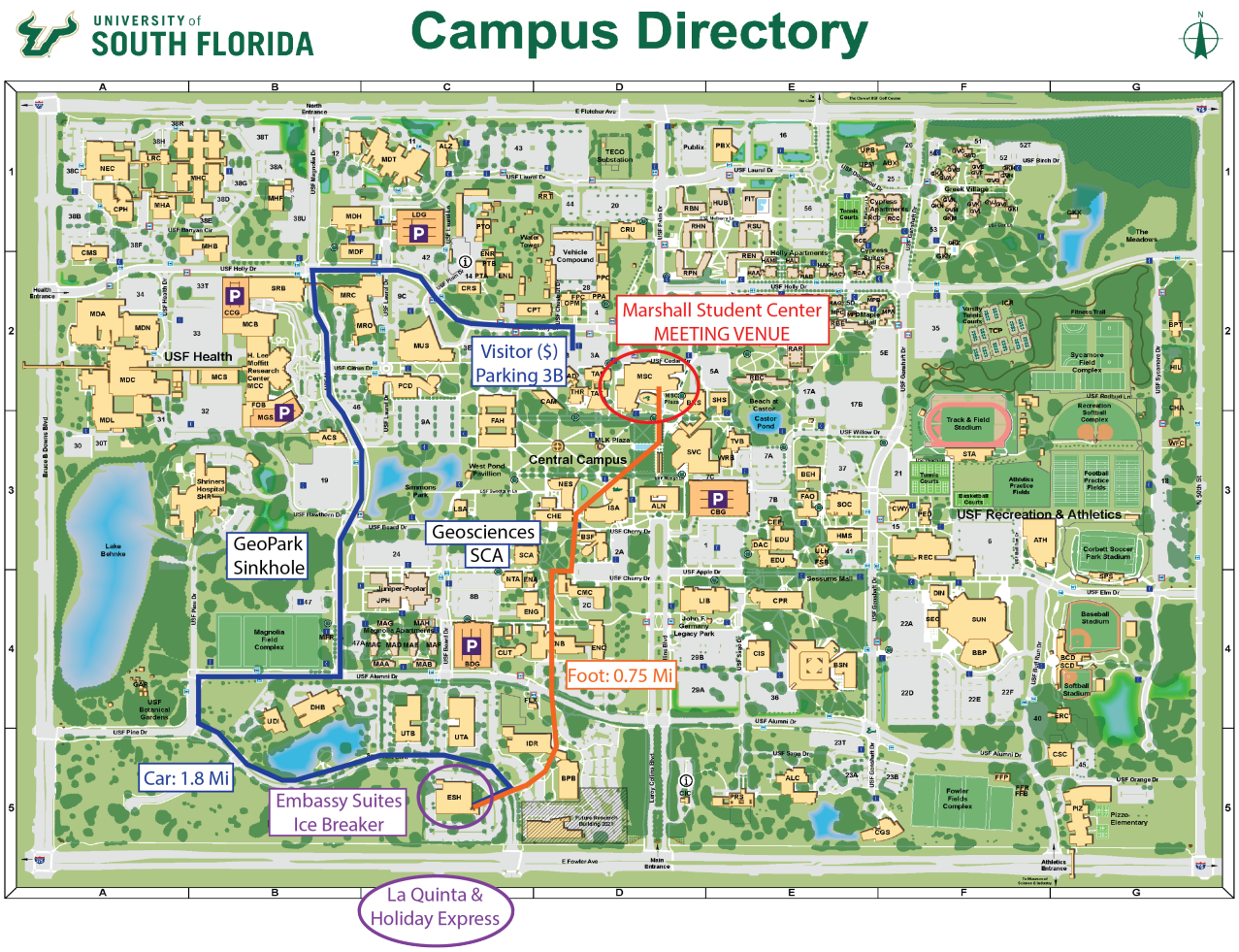

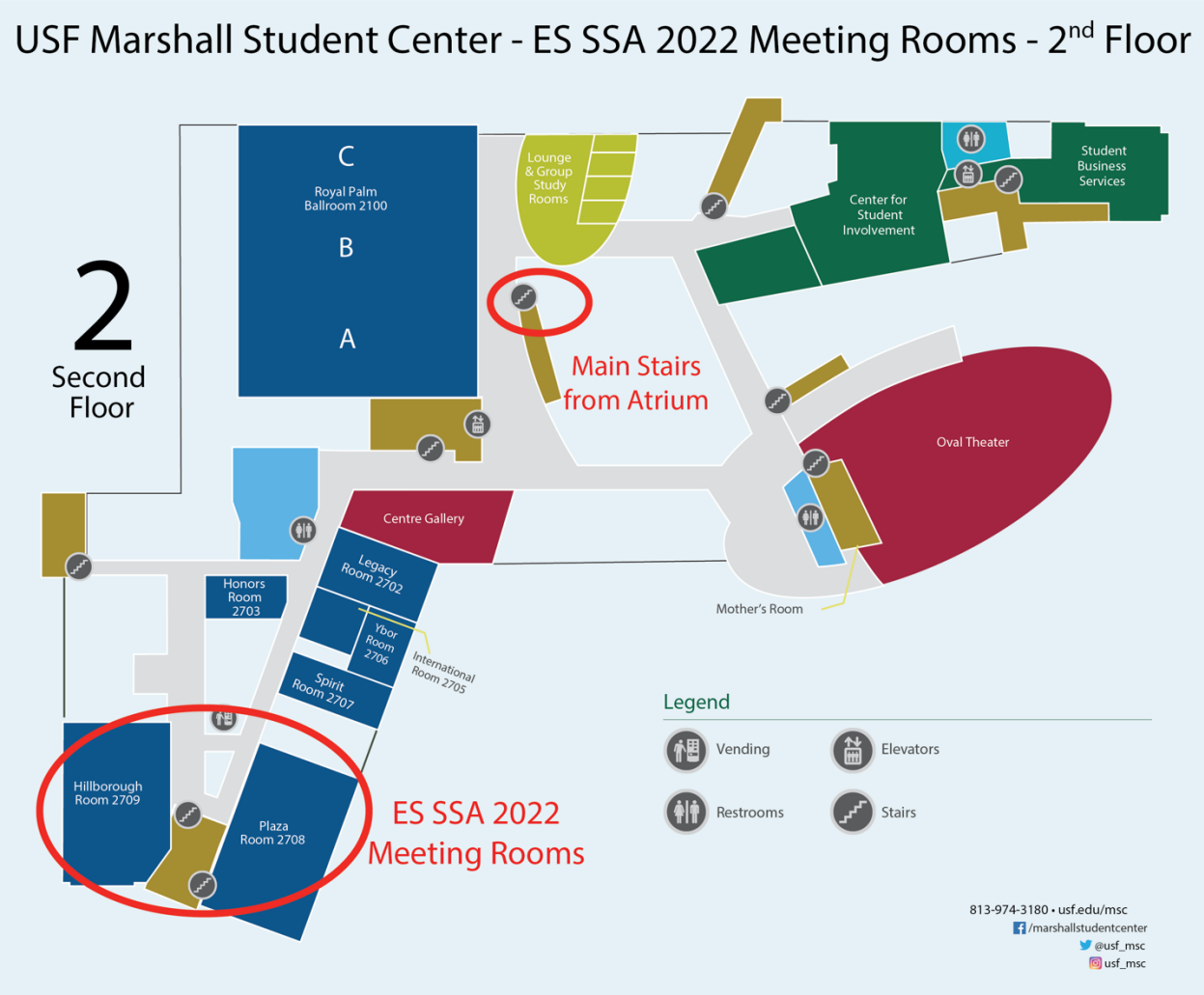
USF Marshall Student Center - ES SSA 2022 Meeting Rooms - 2nd Floor
2
Second Floor
C
Royal Palm Ballroom 2100
B
A
Lounge & Group Study Rooms
Center for Student Involvement
Student Business Services
Main Stairs from Atrium
Oval Theater
Centre Gallery
Legacy Room 2702
Honors Room 2703
Ybor Room 2706
International Room 2705
Spirit Room 2707
Mother's Room
Hillborough Room 2709
Plaza Room 2708
ES SSA 2022 Meeting Rooms
Legend
Vending
Elevators
Restrooms
Stairs
813-974-3180 • usf.edu/msc
/marshallstudentcenter
@usf_msc
usf_msc

Meeting At a Glance

Sunday, October 23	Monday, October 24	Tuesday, October 25
	Registration & Coffee	Registration & Coffee
Field Trip (9:00 - 16:30 or so) lunch provided	Opening Remarks (8:30 - 8:40) **Oral Session M1** (8:40 - 10:00)	**Oral Session T1** (8:20 - 10:00)
	Break & Coffee	Break & Coffee
	Oral Session M2 (10:20 - 12:00)	**Oral Session T2** (10:20 - 11:40)
		Business Meeting
	Lunch (12:00 - 13:30)	Lunch (12:00 - 13:30)
	Oral Session M2 (13:30 - 15:10)	**Poster Session P2** (13:30 - 14:50)
		Break & Coffee
	Coffee **Poster Session P1** (15:10 - 17:00)	**Oral Session T3** (15:10 - 16:30) Closing Remarks Student Awards, Raffle (16:30 - 16:45)
Icebreaker Reception (18:00 - 20:00) Board Meeting (closed, 20:00 - 21:00)	Reception (6 - 7 pm) **Banquet** & Jesuit Society Award Dinner (19:00 - 21:00)	
Venue:	**Embassy Suite** (leave from)	**Embassy Suite**	**Marshall Student Center 2708-2709**

Program

Student presentations are denoted with * before the title; presenting author in **bold**.

Sunday, October 23	
9:00 – 16:30	**Field Trip**. Meet at 8:45 in the lobby of the Embassy Suites
18:00 – 20:00	**Icebreaker Reception** in the Embassy Suites
20:00 – 21:00	Executive Meeting of ES-SSA Officers (private)

Monday, October 24 Meeting Venue: Marshall Student Center MSC – rooms 2708 & 2709	
7:30 – 8:30	**Registration** and Coffee
8:30 – 10:00	**Opening Remarks and Session M1: Earthquake Early Warning & Charlevoix Seismic Zone** ***Chairs: Rogers & Walter***
8:30	Opening Remarks. Stephen McNutt and Jochen Braunmiller.
8:40	Event playback and real-time performance of Earthquake Early Warning in Eastern Canada. **Stephen J. Crane**, B. Angheluta, H. K. C. Perry.
9:00	Integrating the Pick Coda Classifier into routine seismic event detection at Natural Resources Canada. S. Crane, N. Ackerley, **Mareike Adams**, C. Boucher.
9:20	A long-term context for the AD 1663 Charlevoix earthquake interpreted from the post-glacial landslide record in the Gouffre Valley, southern Quebec, Canada. **Greg R. Brooks**, D. Perret.
9:40	Quantify earthquake source parameters and stress field in the Charlevoix Seismic Zone of eastern Canada. **Yajing Liu**, J. Onwuemeka, A. Verdecchia, H. Yu, R. M. Harrington.
10:00 – 10:20	Break & Coffee
10:20 – 12:00	**Session M2: Seismicity and Earthquake Sources in CEUS.** ***Chairs: Gable & Goebel***
10:20	*Earthquake source parameter inversion in the western Quebec Seismic Zone. **Justin Chien**, Andres Felipe Peña Castro, Yajing Liu.
10:40	The earthquake swarms of Eastern Maine and nearby New Brunswick. **John E. Ebel**.
11:00	Gravity, stress analyses, and aftershocks of the 2020 M5.1 Sparta, NC earthquake suggest near-surface slip partitioning and reactivated secondary fault systems at multiple scales. **Will Levandowski**.
11:20	*Using a high-resolution earthquake catalog to unravel the M_w5.1 Sparta, North Carolina, earthquake sequence. **Miguel Neves**, L. Chuang, W. Li, Z. Peng, S. Ni.
11:40	The December 2021-August (?) 2022 Elgin-Lugoff, South Carolina, earthquake swarm. **Steven Jaume**, S. Howard, R. Morrow, S. White, P. Talwani, A. Shah.
12:00 – 13:30	Lunch
13:30 – 15:10	**Session M3: New Madrid Fault Zone and Induced Seismicity.** ***Chairs: Ng & Liu***
13:30	An initial look at the data from the Embayment Seismic Excitation Experiment 2022. **Charles A. Langston**, G. Kaip, Z. Farajpour, S. M. A. Islam, C. Opara.
13:50	New crustal velocity models and earthquake relocations for the New Madrid Seismic Zone. **Christine A. Powell**, C. A. Langston, M.M. Withers.
14:10	Updated fault model for the New Madrid Seismic zone inferred from seismicity clustering. **Charles A. Langston**, C. A. Powell, M. M. Withers.
14:30	An overview of recent injection induced seismicity in the Central and Eastern United States. **Michael R. Brudzinski**, S. E. Fasola, B. C. Currie.
14:50	*Application of a new workflow to re-estimate magnitudes and evaluate variations in b-value for induced seismicity in Oklahoma and Texas. **Sydney Gable**, Y. Huang.
15:10 – 15:30	Break & Coffee
15:10 – 17:00	POSTERS (see complete list at end of Program section

Monday, October 24 Banquet Dinner: Embassy Suites – Salon A, B, C	
18:00 – 19:00	Reception
19:00 – 21:00	**Banquet Dinner** **Jesuit Seismological Association Award** **Banquet Presentation Dr. Mark Rains**, Chief Science Officer of the State of Florida, Professor, School of Geosciences, USF.

Tuesday, October 25 Meeting Venue: Marshall Student Center MSC – rooms 2708 & 2709	
7:30 – 8:20	**Registration** and Coffee
8:20 – 10:00	**T1: Fault Slip Behavior and Earthquake Physics. *Chairs: Sedaghat & Powell***
8:20	Characterization of earthquake clusters and swarm behavior in southern Mexico. **Michael R. Brudzinski**, A. Bennett, W. Ventura-Valentin, S. Graham, E. Cabral-Cano
8:40	Fault roughness promotes earthquake-like aftershock clustering in the lab. **Thomas H. W. Goebel**, E. Brodsky, G. Dresen.
9:00	*Seismic magnitude clustering is prevalent in field and laboratory catalogs. **Derreck Gossett**, M. R. Brudzinski, Q. Xiong, Q. Lin, J. C. Hampton.
9:20	An initial examination on annual variations of seismicity at two intraplate regions. **Zhigang Peng**, Yanyan Zhang, Lingling Ye, Phuc Mach, Miguel Neves.
9:40	Moment tensor uncertainty analysis for the 2017 Hojedk seismic sequence in Iran. **Félix Rodriguez Cardozo**, J. Braunmiller, G. Thompson.
10:00 – 10:20	Break & Coffee
10:20 – 12:00	**Session T2: Site Response. Chairs: *Kayastha & Cardozo***
10:20	Impedance ratios as predictors of primary ground-motion site response characteristics at Central and Eastern U.S. seismic stations. **N. Seth Carpenter**, Z. Wang.
10:40	*Site characterization in New England using high resolution geology maps and a subregion grouping layer. **Marshall A. Pontrelli**, L. G. Baise, J. E. Ebel.
11:00	*Shear-wave velocity profiles for obtaining amplification factors for reference site to local site conditions in the Blue Ridge and Piedmont provinces of South Carolina. **Ali Sedaghat**, R. Andrus, C. Amevorku, I. Wong, G. Rix, C. Carlson, N. Ravichandran, V. S. Jella, N. Harman.
11:20	*Seismic soil-structure interaction analysis of building subjected to different earthquake ground motions. **Abdul Ahad Faizan**, O. Kirtel.
11:40 – 12:00	Business Meeting
12:00 – 13:30	Lunch
13:30 – 14:50	POSTERS (see complete list at end of Program section
14:50 – 15:10	Break & Coffee
15:10 – 16:30	**Session T3: Sensor Noise; Anisotropy; Florida. Chairs: *Pontrelli & Adams***
15:10	*Quantifying seismic noise change in urban and rural regions in Québec, Canada. **Lan Xi Zhu**, Y. Liu, A. F. Peña Castro.
15:30	*Seismic anisotropy beneath the Eastern North American Margin from frequency-dependent shear wave splitting analyses. **Rajani Shrestha**, C. Lynner.
15:50	Study of construction-induced subsidence in South Florida's young limestone using InSAR. **Farzaneh Aziz Zanjani**, F. C. Amelung, K. Sobhan, S. Mirzaee, E. Andiroglu, A. Nanni, N. M. Jean-Louis, I. Moise, A. Sarafraz.
16:10	Tsunami modeling of a new seismic source on the north shore of Cuba. **Stephen R. McNutt**, E. Suleimani.
16:30 – 16:45	Student Presentation Awards (Zhigang Peng) Closing Remarks (Stephen McNutt, Jochen Braunmiller)
16:45	Adjourn

Posters

Up all meeting- Poster Sessions: Mo 15:10 – 17:00 & Tuesday 13:30 – 14:50

Meeting Venue: Marshall Student Center MSC – rooms 2708 & 2709

*****Preliminary relocation results from a temporary seismic deployment around the source zone of the 1886 M 7 South Carolina earthquake. W. Chen, **Miguel Neves**, C. Daniels, Q. Zhai, S. Jaume, Z. Peng.

Classifying seismic events located in the North Central and Northeastern United States by EarthScope's Array Network Facility using Machine Learning. **Jonathan Schmidt**, N. S. Carpenter, Z. Wang.

Anomalous crustal stress in the Eastern Tennessee Seismic Zone. **Will Levandowski**, C. Powell, M. Chapman, Q. Wu.

Void detection using distributed acoustic sensing ambient noise interferometry. M. Mirzanejad, D. O'Connell, M. Isaacson, **Will Levandowski**, J. Nuttall.

Accelerated coastal erosion at Kennedy Space Center: how do seismo-acoustic waves from rocket launches affect groundwater movement? **Glenn Thompson**, S. Krupa, K. Locher, and K. Blair.

A pipeline for near-real-time seismo-acoustic monitoring of quarry blasts in the Miami Lakes region. **Glenn Thompson**, J. Braunmiller, S. McNutt, F. Rodriguez Cardozo, M. Hastings, E. Moslemi.

*****Near-surface P-wave velocity near West Miami, Florida from quarry blast records. **Elham Moslemi**, S. McNutt, G. Thompson, J. Braunmiller.

Accuracy considerations in the implementation of deep-learning earthquake detection. **Jacob I. Walter**, P. Ogwari.

*High resolution site response to Northern Oklahoma using dense Nodal array and its relationship to the shallow subsurface. **Raymond Ng**, X. Chen, N. Nakata, D. Dangwal.

*Fundamental site resonance frequencies in the Upper Mississippi Embayment from ambient noise HVSR using 5 Hz Nodal geophones. **Russel Rogers**, S. Carpenter, Z. Wang.

*Effect of sigma variability due to distance conversion in PSHA. **Melish Kayastha**, S. Pezeshk, B. Tavakoli.

That's the way the Raspberry Shakes: 2022 update on the intriguing variety of things we record with Shakes and Booms. A. L. Kafka, J. J. Pulli, K. R. Fink, C. Stapels, K. Cannon, D. McCasland, K. McLaughlin, R. Block, **Stephen R. McNutt**, J. N. Kafka, M. J. Sharkey.

Hydrological loading deformation and stress changes in the Great Lakes region. **Yuning Fu**, L. Xue, H. R. Martens, Y. Huang.

Abstracts

Abstracts are in alphabetical order of first author's last name. * Indicates student presentation. Presenting author in **bold**. *O* and *P* in front of title indicates presentation type (oral, poster)

O 1. Study of construction-induced subsidence in South Florida's young limestone using InSAR
Farzaneh Aziz Zanjani (University of Miami, fzanjani@earth.miami.edu), F. C. Amelung (University of Miami), K. Sobhan (Florida Atlantic University), S. Mirzaee (Caltech), E. Andiroglu (University of Miami), A. Nanni (University of Miami), N. M. Jean-Louis (University of Miami), I. Moise (University of Miami), and A. Sarafraz (University of Miami)

The tragic collapse of the Champlain South Condominium Tower in Surfside, Florida, motivated examining building's stability and coastal subsidence using space-based interferometric synthetic aperture radar (InSAR). The 2016-2021 Sentinel-1 InSAR data of the towns of Surfside and Bal Harbour in Miami Beach, FL, reveals several subsidence hotspots, including the Surf Club hotel, Oceana, and 87 Park Tower, where construction was completed in 2016, 2016, and 2019, respectively. The subsidence of up to 100 mm over several years following the construction is centered in newly constructed high-rise buildings. For the Surf Club hotel, there was ~40 mm/yr subsidence in radar line-of-sight direction until early 2018, when it leveled out. The temporal correlation of subsidence with nearby construction suggests that the subsidence could be related to the construction of the foundation (e.g., vibration activities). Another building constructed 500 meters north of the Surf Club hotel in 2016 does not show any subsidence. For the Oceana, subsidence continues as of 2022. InSAR data also shows 20 mm of subsidence for the 87 Park Tower, nearby the collapse location. The geotechnical report from 87 Park Tower construction shows interbedded sand layers within the limestone. Therefore, we hypothesize that the subsidence is caused by creep and/or dynamic settlement of these interbedded sand layers. The next steps are to obtain and use the geotechnical reports from the construction of the buildings to compare the underlying soil strata condition to shed light on the lithology of these sites and information on vibration activities. With this information, we will investigate the coupled effect of creep due to sustained loading by new buildings and dynamic settlement from vibrations to explain the diversity in the InSAR signal.

O 2. A long-term context for the AD 1663 Charlevoix earthquake interpreted from the post-glacial landslide record in the Gouffre Valley, southern Quebec, Canada
Greg R. Brooks (Geological Survey of Canada, Ottawa, greg.brooks@nrcan-rncan.gc.ca) and D. Perret (Geological Survey of Canada, Quebec)

Previous research has linked earthflow-earthspread deposits within parts of Gouffre Valley, southern Quebec, to failures triggered by the AD 1663 M 7.5±0.45 Charlevoix earthquake, demonstrating a close connection between landsliding and strong earthquake shaking. This study examined the distribution, stratigraphy, and chronology of the landslide deposits within the greater valley to provide a long-term context for the AD 1663 earthquake. Our mapping utilized a 1x1 m digital terrain model, and we interpreted deposit age and stratigraphy from 23 new AMS radiocarbon ages, supplemented by 49 regular radiocarbon ages and 23 dendrochronology ages compiled from previous studies. These data provide a robust connection between the AD 1663 earthquake and large-scale landslide deposits that extend along about 20 km of the valley bottom and originated from separate source areas. Eight, relatively small-scale, prehistoric landslide features are also present in Gouffre Valley, including three deposits aged between about 7950-7300, 6595-6087, and 1310-1210 cal BC, a poorly constrained deposit aged between 4782-4452 cal BC and AD 1663, three undated landslides, and an undated amphitheatre-shaped landslide source area. There is no evidence to support an earthquake trigger for any of these pre-AD 1663 landslides. Instead, the widespread deposits associated with the AD 1663 earthquake represent the only multi-event, landslide signature in Gouffre Valley. This, in combination with a long gap between early postglacial and late Holocene mass movement activity in several nearby lakes, is

consistent with the AD 1663 earthquake being the largest to occur in the Charlevoix-Kamouraska Seismic Zone since about 7950 cal BC.

O 3. An overview of recent injection induced seismicity in the Central and Eastern United States
Michael R. Brudzinski (Miami University, brudzimr@miamioh.edu), S. E. Fasola, and B. C. Currie

The sharp increase in earthquakes in the Central and Eastern United States over the past decade has primarily been attributed to large volume fluid injection associated with enhanced oil and gas recovery. In this presentation, we will provide an overview of the findings from various studies characterizing human-induced seismicity across the region with comparisons to tectonic seismicity. The majority of induced seismicity and the largest magnitude earthquakes have been the result of disposal of produced and flowback water, but there has also been a prominent amount of seismicity caused directly by hydraulic fracture stimulations. Proximity of fluid injection to mature faults optimally oriented in the stress field appears to be a key ingredient for generating seismicity. However, fault identification can be difficult prior to injection, particularly in the predominantly strike-slip settings. Observational studies point to the injection flux (volume per area per time) being a key factor raising the likelihood of induced seismicity. This is supported by modeling studies that identify the seismicity rate being driven by the rate of change in pore fluid pressure. These findings provide some guidance in terms of best practices for mitigating the hazard via regulatory and operational strategies, but ultimately broader integration with geomechanical, hydrological, and structural datasets will be necessary. It will be important to continue to learn lessons from the ongoing large-scale fluid injection "experiment" to better understand the hazards associated with even larger volume injection that will be necessary to make carbon sequestration economically viable.

O 4. Characterization of earthquake clusters and swarm behavior in southern Mexico
Michael R. Brudzinski (Miami University, brudzimr@miamioh.edu), A. Bennett, W. Ventura-Valentin, S. Graham, and E. Cabral-Cano

The Mexican subduction zone is considered a natural laboratory for studying slip processes due to the relatively short (~50 km) trench-to-coast distance which brings broad portions of the seismogenic and transition zones ~250 km inland. Slow slip events (SSEs) have been identified to occur downdip of the megathrust seismogenic zone where the friction style changes from stick-slip to stable sliding. A recent study by Fasola et al. (2019) found that correlated SSEs and seismicity in the Oaxaca Region also occurred on a crustal sliver fault that accommodates the partitioning of oblique convergence in Mexico. Hence, this region provides an opportunity to pursue a detailed characterization of potential relationships between the seismicity and aseismic slip on a complex fault plate boundary system. In this study, we will characterize swarms and aftershock sequences recorded by the SSN since 2008 by identifying earthquake clusters based on nearest-neighbor distances of events in the space-time-energy domain (Zaliapin and Yehuda Ben-Zion, 2013). In addition, we demonstrate the utility of waveform correlation primarily focused on earthquake swarms associated with the sliver fault to enhance the detection of smaller magnitude sequences not identified by the original catalog. This allows us to improve the detection of fluctuations in seismicity rates and their potential relationships to processes identified in geodetic data such as SSE or variations in interseismic coupling.

O 5. Moment tensor uncertainty analysis for the 2017 Hojedk seismic sequence in Iran
Félix Rodriguez Cardozo (felixr1@usf.edu), J. Braunmiller, and G. Thompson (all University of South Florida)

In December 2017, a sequence of strong earthquakes occurred in the Hojedk region of southeastern Iran. Interestingly, the sequence consisted of three 'main' events with magnitude M_w near 6.0 (Savidge et al., 2019; Niazpour et al., 2020) that were followed by a vigorous aftershock sequence. Braunmiller et al. (2019) reported deviatoric moment tensors for about 50 events of the sequence from inversion of long-period regional waveforms with depth estimated by grid search. Waveform inversion provides a 'best-fit' solution of seismic

source parameters but does not per se provide parameter uncertainties. Waveforms change smoothly with variations in source parameters suggesting that parameter uncertainties and trade-offs might be significant. Here, we used the Moment Tensor Uncertainty Quantification code (MTUQ) that performs grid-searches over the double couple and full moment tensor space to gain insights into the parameter resolution of the seismic moment tensors as a function of event size, station coverage, centroid depth, and frequency band used for analysis. The Hojedk sequence is an excellent test case as events cover a range of sizes and station coverage is good. Uncertainty quantification is key to reliable event discrimination and to improve tectonic interpretation of earthquake focal mechanisms.

O 6. Impedance ratios as predictors of primary ground-motion site response characteristics at Central and Eastern U.S. seismic stations

N. Seth Carpenter (University of Kentucky, seth.carpenter@uky.edu) and Z. Wang (University of Kentucky)

Earthquake shear waves can become trapped between the free surface and high-impedance basal layers resulting in additional amplification at specific frequencies. This shear-wave-resonance phenomenon is a primary concern for mitigating ground-motion site response. The standard approach to quantifying resonance-dominated site response involves 1D analyses that require detailed velocity models. Thus, developing one or more simple and reliable proxies to quantify site resonance is desirable. We evaluated the relationship between impedance ratios determined from site shear-wave velocity profiles and the fundamental and peak resonance frequencies and amplifications at 43 seismic stations in the central and eastern U.S. The impedance ratios were calculated as the ratio of the impedance of the base layer to the average impedance of the overlying layers. We found that the depths to bedrock and to the maximum impedance ratios most skillfully predict the frequencies of the first and peak modes, respectively, determined from 1D linear response analyses. Also, we found that theoretical 1D fundamental-mode amplifications are well predicted by bedrock-to-average-sediment impedance ratios and that maximum impedance ratios best predict peak theoretical amplifications.

***P 7. Preliminary relocation results from a temporary seismic deployment around the source zone of the 1886 M 7 South Carolina earthquake**

W. Chen (University of Minnesota), **Miguel Neves** (Georgia Tech, mjneves@gatech.edu), C. Daniels (ARA Inc.), Q. Zhai (Caltech), S. Jaume (College of Charleston), and Z. Peng (Georgia Tech)

The 1886 magnitude ~7 Summerville, South Carolina earthquake was the largest recorded on the east coast of the United States. A better understanding of this earthquake would allow for better evaluation of the intraplate seismic hazard in this region. However, due to a lack of seismic observations from the time and lack of distinctive surface rupture, the fault structure remains unclear. A previous study based on results from a 2011-2012 deployment of seismometers has suggested a south-striking west-dipping zone of modern seismicity in the region which is contended by other geophysical studies. Starting in May 2021, a temporary 19-station short-period network was deployed in the Summerville region. We use the network to identify more events and better interpret the spatial variations in microseismicity in the region. Starting with 52 template events, including two magnitude ~3 events on September 27, 2021, we perform a matched filter detection with the one year of continuous data from this deployment along with data from four permanent stations, resulting in over 170 total event detections. We then determine precise relative locations of a portion of these events using differential travel-time relocation methods and compare the results with that of the previous 2011-2012 deployment. The best relocation method returned a relocate catalog of 164 events. We also determine focal mechanism solutions for three events from September 27, 2021 with magnitudes 2.0, 3.1, and 3.3 and infer their fault planes from the relocation results. Our preliminary results also illuminate a south-striking west-dipping zone in the southern seismicity cluster, which is consistent with the thrust focal mechanism of the magnitude 3.3 earthquake on September 27, 2021. In comparison, the northern seismicity cluster likely occurs on a north-south striking right-lateral strike-slip fault, consistent with previous results and complex patterns of stress and faulting expected in the region.

***O 8. Earthquake source parameter inversion in the western Quebec Seismic Zone**

Justin Chien (McGill University, shihhan.chien@mail.mcgill.ca), Andres Felipe Peña Castro (University of New Mexico), and Yajing Liu (McGill University)

The Western Québec Seismic Zone (WQSZ) is one of the most active seismic zones in eastern Canada that encloses the Ottawa Valley from Montréal to Témiscaming and from Cornwall up along the Laurentian Mountains. Although the WQSZ has historically experienced earthquakes as large as the 1935 M 6.2 Témiscaming earthquake, detailed, high-resolution earthquake source parameters and a comprehensive active fault database are not yet available. In this study, we first perform an automatic earthquake phase detection based on a multi-task deep neural network and associate events by the phase pick number as well as travel time residual. Next, we use a least-square maximum likelihood location method to determine the initial event locations followed by the double-difference (DD) relocation. Our results successfully enhance the Natural Resources Canada (NRCan) catalog from ~200 events to ~1500 events in a nearly four years period that provide adequate station distribution (the United States transportable seismic array from 2013 to 2015, Canadian seismic array from 2020 to 2022) in the Greater Montréal area. More importantly, the relocated seismicity forms several local clusters near the Greater Montréal area, indicating the presence of local active fault structures. We further calculate event source parameters, including the focal mechanism solution (FMS) and stress drop estimates. High-resolution seismicity distribution can highlight previously unmapped but seismically active faults, and FMSs help constrains fault orientations and stress field inversion. The inferred fault orientation and the static stress drop estimate provide critical source property constraints to implement finite fault slip models in seismic hazard and risk assessment models.

O 9. Event playback and real-time performance of Earthquake Early Warning in Eastern Canada

Stephen J. Crane (stephen.crane@nrcan-rncan.gc.ca), B. Angheluta (Natural Resources Canada), and H. K. C. Perry (all Natural Resources Canada)

Natural Resources Canada (NRCan) is deploying a national Earthquake Early Warning (EEW) system for regions of high-to-moderate seismic risk. Eastern Canada has significant population centers with possible exposure to large and potentially damaging earthquakes. The large earthquakes, although infrequent, have the potential to disrupt significant areas of eastern Canada due to low attenuation of seismic energy. This low attenuation relative to western North America in turn means that warnings may be issued for areas 1.5-6 times larger than in the west. Since the station density and speed to generate alerts is expected to be similar between the regions, not only will larger areas be alerted for a given intensity, but those populations should generally get larger warning times. NRCan, in collaboration with the United States Geological Survey (USGS), has been running an adapted version of the USGS ShakeAlertTM software in eastern Canada since May 2022. Real-time waveform data recorded by Canadian National Seismic Network (CNSN) seismic stations in eastern North America are input into this software, producing rapid estimates of the source parameters of earthquakes. To test the performance of the EEW system in eastern Canada, a suite of CNSN-recorded seismic events were identified and their waveform data replayed through the USGS ShakeAlertTM software. In this presentation, we show that with minimal changes to the configurations and parameters of the software, events with sufficient near-source recordings generally produce timely and accurate epicenters. Various magnitude relationships were tested, and we show an eastern Canada specific relationship was developed and found to improve magnitude accuracy. The speed of event alerting, and the quality of the alerts, from the planned EEWS is expected to increase as the CNSN network station inputs are replaced by the significantly denser and lower latency EEW network.

O 10. Integrating the Pick Coda Classifier into routine seismic event detection at Natural Resources Canada
S. Crane, N. Ackerley, **Mareike Adams** (mareike.adams@nrcan-rncan.gc.ca), and C. Boucher (all Natural Resources Canada)

The Pick Coda Classifier (PCC) is an automated routine designed to identify seismic properties in signals recorded by the Canadian National Seismograph Network (CNSN). An update to the Unlocated Event Filter (ULF), the PCC was integrated into SeisComP to replicate the legacy methods of automated seismic event detection at Natural Resources Canada (NRCan) as the software and hardware of these systems are continually updated. In eastern Canada there are many picks recorded by the CNSN sensors, with the vast majority being non-seismic in origin. At the same time, many small seismic events produce an insufficient number of picks to pass the quality check for automatic detection. Thus systems like ULF, and now PCC, are crucial for maintaining the catalogued magnitude of completeness in Canada. The PCC is implemented in near real-time, since it requires waveform data before and after the pick. In order to determine if a pick is suspected of being seismic the PCC, similar to the ULF, pre-processes the waveform data then estimates the slope and duration of the coda wave. If these fall within predefined thresholds, the PCC will classify the pick as seismic. The seismic picks that remain unassociated with automatically generated seismic events are collected into a web interface for analyst review. We performed a study to validate the results of the implementation of the PCC. Here, we present the results of this study, and as well describe our routine seismic event detection workflow. Finally, we discuss potential future improvements to our system.

O 11. The earthquake swarms of Eastern Maine and nearby New Brunswick
John E. Ebel (Weston Observatory of Boston College, ebel@bc.edu)

In the past couple decades, several swarms of small earthquakes have been detected in eastern Maine and nearby New Brunswick. The swarms were near Bar Harbor, Maine in 2006-2007, at Searsport, Maine in 2011, at McAdam, New Brunswick in 2018 and near Jonesboro, Maine in summer 2022. Each swarm has consisted of several to a few dozen events, with the largest event in any of the swarms being an MLg 4.2 earthquake near Bar Harbor in 2006. Relative locations of the events in the swarms suggest that they are only one or a couple kilometers in spatial extent and that they tend to follow known or inferred local geologic structures. The focal mechanisms of the largest events of the swarms indicate that the earthquakes in these swarms are responding to the regional approximate E-W maximum compressive field seen throughout Maine, and the events tend to have thrust focal mechanisms. The swarms all have focal depths of a few kilometers or less. The swarms do not associate with any single structure or structural trend, although they all have occurred just east of or on the Norumbega Fault, an ancient, major strike-slip fault that runs from eastern New Brunswick southwest to near the southern tip of Maine. The causes of these swarms are unclear, as is their significance for elucidating the earthquake hazard of the region.

***O 12. Seismic soil-structure interaction analysis of building subjected to different earthquake ground motions**
Abdul Ahad Faizan (Sakarya University of Applied Sciences, ahad.faizan@ogr.sakarya.edu.tr) and Osman Kirtel (Sakarya University of Applied Sciences)

During earthquakes, seismic waves propagate from the bedrock through the soil layers and damage structures located on the surface. Therefore, understanding the local site effects on strong ground motion is of particular importance for future earthquake-resistant design and mitigation of earthquake disasters. In this paper, the seismic response of a reinforced concrete structure under different earthquake ground motions considering soil-structure interaction (SSI) is investigated. In this study, the characteristics of input motions and local soil conditions are important parameters for numerical simulation and seismic analysis. The analysis was performed by considering three actual ground motion records representing seismic motions with different frequency content earthquakes. Three types of earthquakes including Loma Prieta (USA, 1989), Kobe (Japan,

1995) and Kocaeli (Turkey, 1999) earthquakes were used as input motions in the seismic analysis. Considering the soil property of the building site, analysis was done for three types of soil which are defined as soft, medium, and rock. An advanced 2D finite element model of the soil-structure system was established with the Mohr-Coulomb failure criterion under plane-strain conditions. Dynamic analysis of the proposed structure-soil coupled model was performed in the time domain using the Plaxis program. To minimize the artificial reflections and to dissipate the vibrational energy at the boundaries, the lateral extension of the infinite domain is modelled by viscous absorbing boundaries. According to the result of the dynamic analysis, the dynamic responses of the structure including element forces, displacements, and accelerations are calculated and shown in graphic forms. The analysis which is obtained by the Loma Prieta earthquake is compared with the results obtained by the Kobe and Kocaeli earthquakes for different soil conditions. It is seen that the dynamic responses are different for each kind of earthquake ground motion, hence it means that the structure and soil have different responses to various kinds of earthquake ground motions. The numerical analysis demonstrated that the displacements values are increasing dramatically from hard rock to soft soil. Results illustrate that the proximity of the fundamental frequencies of the structure, soil, and earthquake strongly influences SSI. Therefore, the phenomenon of structural soil interaction must be considered in the building seismic analysis.

P 13. Hydrological loading deformation and stress changes in the Great Lakes region

Yuning Fu (Bowling Green State University, yfu@bgsu.edu), L. Xue (Syracuse University), H. R. Martens (University of Montana), and Y. Huang (University of Michigan)

The water mass variations in the Great Lakes result in surface elastic loading displacements and subsurface stress changes in the surrounding area. We use a finite element model to compute the hydrologically induced loading response of the lithosphere in the central mid-east region of North America to the surface water mass variations (e.g., lake water, snow, and soil moisture). The comparison with GNSS observation indicates that seasonal deformation in the Great Lake region measured by GNSS is dominated by regional-scale hydrological loading, with the correlation coefficients larger than 0.9 for some stations close to the lakes but vary spatially in the whole Great Lakes basin. We also apply different Earth structures, including the ones with lateral variations, to investigate the sensitivities of the loading response to Earth models. Our result indicates that the structural variations have very small impact (<0.2 mm) on the modeled hydrological loading displacements. In addition, we calculate the loading stress changes on the potential fault that hosted the 2019 M=4.0 Ohio earthquake, and find that the Coulomb stress change is not only related to lake water mass change, but also highly depends on the frictional coefficients.

***O 14. Application of a new workflow to re-estimate magnitudes and evaluate variations in b-value for induced seismicity in Oklahoma and Texas**

Sydney Gable (University of Michigan, gablesyd@umich.edu) and Y. Huang (University of Michigan)

Subsurface fluid injection related to high-volume wastewater disposal and hydraulic fracturing are two commonplace industrial activities currently taking place in the central and eastern United States. These processes are often linked to increased seismic activity that causes nuisance and potential hazard in certain locations such as central Oklahoma in the early 2010's and currently the Permian Basin region of western Texas and southeast New Mexico. In order to mitigate the seismicity that is produced as a result of these activities, we must understand how the seismic sequences evolve in response to injection. Unlike natural tectonic sequences, we cannot use past seismic records to infer future induced seismicity forecasts or hazard estimates as injection parameters are constantly changing. Therefore, new approaches that can evaluate changes in seismicity over short or near-real time scales are required. We present a multi-step workflow designed to re-estimate the magnitudes associated with these earthquakes and evaluate the temporal and spatially dependent variations in MFD and the b-value. We then relate these variations to the locations and timing of the largest induced events. The first major step in our workflow is to re-estimate earthquake magnitude using

a relative magnitude method based on relative waveform amplitudes. Then we determine temporal and spatial variations in b-value using the positive successive differences in magnitude. We have previously applied this workflow to the 2011 Prague, OK sequence and found overall low b-values and variations indicative of periods with greater likelihood to produce relatively large events. We now apply our methods to the Delaware Basin region, a subset of the greater Permian Basin and present preliminary results for the area. With these results we aim to improve rapid characterization of induced seismicity and address whether b-value may be used to address seismic hazard estimation in near-real time for induced seismicity.

O 15. Fault roughness promotes earthquake-like aftershock clustering in the lab

Thomas H. W. Goebel (University of Memphis, thgoebel@memphis.edu), E. Brodsky (UC Santa Cruz), and G. Dresen (GFZ-Potsdam)

The average behavior of large populations of earthquakes, including aftershocks, is well described by basic statistical relations. However, the prediction of individual aftershock sequences is complicated by poorly understood triggering mechanisms, crustal stresses and fault zone properties. We untangle contributions of stress, fault zone properties and mainshock characteristics to the generation of aftershocks. Seismic sequences are investigated during frictional sliding on rough and smooth faults at mid-crustal stresses in the laboratory. Our experiments lead to complex fault slip behavior including preparatory aseismic slip, stable sliding and dynamic failure, which can be explained by the difference between the rate of strength and stress reduction with slip. Experimental conditions close to frictional instability lead to seismicity statistics (e.g. waiting time and spatial distributions) that are indistinguishable between lab and nature. Smooth faults within the unstable frictional regime produce power-law seismicity rate increase before slip but essentially no aftershocks. Rough faults, on the other hand, favor aseismic deformation before dynamic failure and promote high aftershock productivity, particularly when residual stress after rapid slip events is high. We conclude that seismic sequence partitioning into fore, main and aftershocks is strongly affected by residual stress and fault roughness.

***O 16. Seismic magnitude clustering is prevalent in field and laboratory catalogs**

Derreck Gossett (Miami University, gossetd@miamioh.edu), M. R. Brudzinski (Miami University), Q. Xiong (University of Wisconsin, Madison), Q. Lin (China University of Petroleum), and J. C. Hampton (University of Wisconsin, Madison)

Clustering of earthquake magnitudes is still actively debated, compared to well-established spatial and temporal clustering. Magnitude clustering is not currently implemented in earthquake forecasting but would be important if larger magnitude events are more likely to be followed by similar sized events. Investigating many laboratory and field catalogs, we observed magnitude clustering at a wide range of spatial scales (mm to 1000 km). Filters based on magnitude of completeness and interevent times were applied to address previous study concerns of network detection limitations and short-term aftershock incompleteness. This phenomenon was still observed after various filters were applied, demonstrating that magnitude clustering is not an artifact but a widespread phenomenon. Field results demonstrate it is universal across fault types and tectonic/induced settings, while laboratory results are unaffected by loading protocol or rock types and show temporal stability. The absence of clustering can be imposed by a global tensile stress, although clustering still occurs when isolating to triggered event pairs or spatial patches where shear stress dominates. Both the lab and field analyses found magnitude clustering is most prominent at short time and distance scales, suggesting this is part of the physical process. Synthetic catalog modeling using both ETAS and Gutenberg-Richter probability density methods indicates >20% repeating magnitudes in some cases, implying it can help to narrow physical mechanisms for seismogenesis.

O 17. The December 2021-August (?) 2022 Elgin-Lugoff, South Carolina, earthquake swarm

Steven Jaume (College of Charleston, jaumes@cofc.edu), S. Howard (South Carolina Geological Survey), R. Morrow (South Carolina Geological Survey), S. White (University of South Carolina), P. Talwani (University of South Carolina), and A. Shah (U. S. Geological Survey)

On December 27, 2021, a widely felt M 3.3 earthquake occurred east of Elgin and southwest of Lugoff, South Carolina, starting a 9-month swarm of felt events in an area of low pre-existing seismicity. As of September 15, 2022, this swarm has produced 76 located events, five of which were M 3+ (Dec. 27, 2021 M 3.3; May 9, 2022 M 3.3; June 26, 2022 M 3.4; June 29, 2022 M 3.5 and 3.6). This earthquake swarm has occurred in several pulses, some initiated by one or more M 3+ events, with month-long pauses in between each pulse. These larger events were widely felt in the Midlands of South Carolina, including the state capital Columbia, and the smaller events were regularly felt by local residents, causing considerable concern. New high-resolution aeromagnetic data show that the earthquakes are occurring within the Modoc zone of the Eastern Piedmont fault system where it is buried beneath Atlantic Coastal Plain sediments. The Modoc zone consists of ductile to brittle Paleozoic faults and folds roughly paralleling the Fall Line, and is expressed as a series of narrow (<100 m wide) N55E-N65E-trending magnetic lineaments. The fault system is exposed within the Piedmont Province and continues along strike beneath Atlantic Coastal Plain sediments. Near the recent seismicity, some of these lineaments locally terminate along a >12-km-long, NNE-trending, linear zone that is roughly parallel to and about 1.5 km west of the trend of the swarm. The earthquake swarm thus does not appear to be occurring on any of the main strands of the fault system but rather on a NNE-striking diagonal cross fault. This is also consistent with the focal mechanisms of the larger events, which show a combination of reverse, oblique-reverse and strike-slip faulting with one nodal plane parallel to the strike of the swarm.

P 18. That's the way the Raspberry Shakes: 2022 update on the intriguing variety of things we record with Shakes and Booms

A. L. Kafka (Weston Observatory, Boston College, alan.kafka@bc.edu), J. J. Pulli (Raytheon BBN Technologies), K. R. Fink (Texas Educational Seismic Project), C. Stapels (MathWorks), K. Cannon (Weston Observatory, Boston College), D. McCasland (Blue Hill Observatory and Science Center), K. McLaughlin (Leidos Dynetics-LInC), R. Block (Snow Star Farm), **Stephen R. McNutt** (University of South Florida), J. N. Kafka (WeirdHat.com), and M. J. Sharkey (Boston College)

People usually think of seismographs as recording earthquakes, which of course they do, but they also record lots of other things that “shake”, such as activities of people and vehicle traffic. Seismologists install research seismographs in quiet places so that earthquake signals won’t be obscured by non-earthquake noise. Educational and community seismographs, by contrast, are often purposely installed near human cultural noise sources so that they can be near where the people are, enabling people to interact with them. That can be a problem for monitoring earthquakes, but it’s not always bad for other aspects of seismology, and can sometimes (with appropriate filtering) be less of a problem for earthquakes than might be expected. For the past several years, our group of professional and community seismologists has been exploring what the affordable Raspberry Shakes (seismic) and Booms (infrasound) are recording. Here we present a 2022 update on the intriguing variety of things we record with our Raspberry Shakes and Booms (RSBs). These RSBs, built with a high-frequency geophone integrated with a Raspberry Pi computer, often record earthquakes better than might be expected, and also record a lot of other interesting seismic events, such as: storms, snowplows, wind turbines, street traffic, aircraft, construction sites, thunder, washing machines, volcanoes, and more. We find that RSBs are surprisingly good for recording local and regional earthquakes and that they also record some large, distant earthquakes better than might be expected. Often urban and suburban areas are poorly represented with seismographs, and RSBs can fill in such locations for more uniform spatial monitoring. The growing database of RSB seismograms of earthquakes and an intriguing variety of other types of seismic sources highlights opportunities for community scientists, educators, and research scientists to collaborate in monitoring our active planet.

***P 19. Effect of sigma variability due to distance conversion in PSHA**

Melish Kayastha (The University of Memphis, mkyastha@memphis.edu), S. Pezeshk (The University of Memphis), and B. Tavakoli (Bechtel Corp.)

Probabilistic Seismic Hazard Assessment (PSHA) incorporates different distance metrics to calculate the seismic hazard of an area. To obtain accurate seismic hazard, we need to use consistent distance metric in the PSHA. So, we need to convert different distance metrics to a singular reference distance metric. However, the distance conversion also increases the uncertainty of the ground motion models (GMMs) used in the PSHA. In this study, we provide empirical equations for distance conversion, and for the sigma which can be included in the total uncertainty for the GMM based on standard error propagation techniques. The equations are based on magnitude and dip angle. For a simple PSHA study of a circular area of radius 100 km using Pezeshk et al. (2011), we determined an increase in hazard using the proposed empirical equations and their uncertainties. We compared the sigma variation of our proposed models with other published studies and found the sigma values to be smaller, resulting in a smaller increase in the total variability compared to other models. The proposed empirical equations are developed based on the geometry of the fault and can be used for any GMMs for seismic hazard calculations. We can use the proposed empirical equations for a range of dip angles varying from 10° to 90°, magnitude from 5.0 to 8.0 and distances up to 1000 km.

O 20. Updated fault model for the New Madrid Seismic zone inferred from seismicity clustering

Charles A. Langston (clangstn@memphis.edu), C. A. Powell (University of Memphis), and M. M. Withers (all University of Memphis)

Fault plane models of the New Madrid Seismic Zone developed purely from examining clusters of relocated earthquakes are extrapolated to the Earth's surface and to fault intersections to examine possible correlations with surface geology, past geophysical studies and to guide future seismic experiments in the zone. The hypocenter data come from a recent, high-resolution joint inversion of hypocenters and 3D velocity structure. Individual subclusters of seismicity associated with projected linear features are extracted from the catalog and a plane is fit to the subcluster by computing its covariance matrix. These fault planes determined by hypocenters are then extrapolated to connect with other faults of the model and to the Earth's surface. The Reelfoot fault is seen to have at least 4 major segments with dips of 41 degrees, 27-35 degrees, 37 degrees, and 37 degrees, respectively from north to south. The southern segment of the Reelfoot fault is displaced northeastwards from northern segments at the location of the northeast striking, southwest dipping Ridgely fault. There are two clusters of seismicity immediately to the north of the Ridgely fault, one of which having a similar dip to the southern segment of the Reelfoot fault. The surface expression of this northern segment coincides with the known location of the fault-bend fold associated with the formation of Reelfoot Lake. The less steeply dipping, and largest segment of the northern Reelfoot fault extends to the surface where the Markham fault has been proposed. As in our previous study, we suggest that faults of the New Madrid Seismic Zone are highly segmented suggesting heterogeneous basement structures from a long tectonic history containing different stress states with time.

O 21. An initial look at the data from the Embayment Seismic Excitation Experiment 2022

Charles A. Langston (University of Memphis, clangstn@memphis.edu), G. Kaip (University of Texas, El Paso), Z. Farajpour (University of Memphis), S. M. A. Islam (University of Memphis), and C. Opara (University of Memphis)

Although it has been long recognized that the velocity and attenuation structure of embayment sediments are essential parts of estimating the shaking hazards of earthquakes from the New Madrid seismic zone, it is surprising that there have been few controlled source experiments to examine the entire velocity profile of the sediments or how actual strong and weak motion P, S, and surface waves propagate through them. A passive,

3 km long, reversed refraction profile of 60 nodal seismometers was deployed near Marion, AR, about 20km west of Memphis, TN, from 20 July to 2 August 2022. 200 lb explosives emplaced in 15m deep boreholes were detonated on the nights of 25 and 26 July by personnel of the IRIS Source Facility, University of Texas, El Paso. Additional experiments included collection of small-scale P and SH refraction data near each shotpoint, near-source velocity and acceleration measurement for each explosion, and passive collection of ambient noise data over the duration of the nodal deployment. Scientific objectives include determining self-consistent P and S wave velocity profiles for embayment unconsolidated sediments, depth dependence of P wave and S wave attenuation, characterization of possible non-linear wave propagation in the strong motion near each source, and consistency of ambient noise H/V measurements with the derived velocity and attenuation models. Highlights of the data include measuring over 4g's of acceleration within 50m of the southern shotpoint and display of primary and multiple P and converted phase reflections and refractions within the sediments.

O 22. Gravity, stress analyses, and aftershocks of the 2020 M5.1 Sparta, NC earthquake suggest near-surface slip partitioning and reactivated secondary fault systems at multiple scales
Will Levandowski (Tetra Tech, bouldergeophysics@gmail.com)

The 2020 M_w5.1 Sparta, NC mainshock resulted from remarkably shallow (hypocenter < 1 km) sinistral-reverse slip on the ESE-striking Little River Fault (LRF), causing the first observed surface rupture in the eastern U.S. and more than 300 aftershocks. Regional gravity data shows that the mainshock and aftershock sequence are confined to a high-gravity wedge-shaped structural block but cut across primary NE-striking Paleozoic faults. In fact, the LRF is embedded in previously-identified topographic lineament and a ~75-km-long WNW–ESE-trend of gravity torsion (third horizontal derivative) truncations. Torsion aligns parallel to structural grain, making truncations a sensitive indicator of secondary faulting. The LRF appears to be part of a longer post-Paleozoic structure or deformation zone that cross-cuts primary ancestral faults. The seismically active wedge is bounded to the SW by a parallel trend of torsion truncations and topographic lineament, perhaps indicating a second seismically capable fault system in the region. Near-surface deformation in Sparta also reused inherited secondary faults. Aftershocks—mainly occurred within 10 km of the epicenter, illuminating multiple very shallow, near-vertical, E–W and NNE-SSW strike-slip faults, while coseismic surface deformation mainly comprised NE-vergent dip-slip on low-angle faults: Could these inherited faults have decomposed sinistral-reverse hypocentral motion into strike-slip and dip-slip components in the near-surface? Fault slip potential modeling indicates that the strike-slip faults are nearly optimally oriented in the regional stress field, so their reactivation likely represents typical triggering by stress transfer. Similarly, the spatiotemporal aftershock sequence behavior is average for CEUS sequences, also consistent with typical stress transfer. The Sparta earthquake and its aftershocks piggybacked on multiple sets of inherited faults, yet additional high-resolution, high-precision terrestrial relative gravity data could reveal details of hypocentral structure, aftershock fault network, and the seismogenic potential of the LRF and others in the region.

P 23. Anomalous crustal stress in the Eastern Tennessee Seismic Zone
Will Levandowski (Tetra Tech, bouldergeophysics@gmail.com), C. Powell (CERI/University of Memphis), M. Chapman (Virginia Tech), and Q. Wu (Lettis Consultants International)

The Eastern Tennessee Seismic Zone (ETSZ) experiences the second highest rates of natural seismicity in the central and eastern United States (CEUS), following the New Madrid area. The cause of elevated earthquake rates is unknown but has important implications for seismic hazard. We probe the origin of ETSZ seismicity, using focal mechanism stress inversions to compare the states of stress in the ETSZ and its surroundings. Oblique extension in the ETSZ is unique in the CEUS and cannot be ascribed to (compressive) tectonic plate-boundary forces. A localized source of stress, which apparently overwhelms the regional tectonic stress, is necessary to explain this distinct deformation style. One possible source is gravity-derived stress, related to

isostatic disequilibrium and/or surface processes, may be responsible for the perturbed stress-state. Increased long-term hazard may be controlled by and confined to the spatial extent of this anomalous seismotectonic state. On a methodological note, some of 62 focal mechanisms from the ETSZ—first-motion solutions for older events—are poorly constrained, in that numerous strike/dip/rake combinations explain the polarities equally well. Given an estimate of the stress tensor, however, the angular misfit between the slip vector for each candidate mechanism and the shear traction on that plane can be calculated. The best-fitting mechanism for each event is then selected and inverting these 62 mechanisms gives an updated estimate of the stress tensor, recursively. We show that this approach produces significantly more precise and significantly different results from conventional inversions, including a larger extensional component in the ETSZ. Stress inversions could be helpful in other studies using poorly constrained first-motion focal mechanisms.

O 24. Quantify earthquake source parameters and stress field in the Charlevoix Seismic Zone of eastern Canada

Yajing Liu (McGill University, yajing.liu@mcgill.ca), J. Onwuemeka (Amadeus), A. Verdecchia (Ruhr University Bochum), H. Yu (Pacific Geoscience Centre, Geological Survey of Canada), and R. M. Harrington (Ruhr University Bochum)

The Charlevoix Seismic Zone (CSZ) is located along the St. Lawrence paleorift system between the Grenville Basement and the Appalachian Nappes and overprinted by a Devonian meteorite impact structure. The CSZ hosts the most active seismic zone in eastern Canada, with five M_w 6+ earthquakes reported since the 17th century. Present-day seismicity is generally associated with the reactivation of the late Proterozoic Iapetus rifts. In this presentation, we summarize new findings of CSZ earthquake source properties from our recent works [Yu et al., 2016; Onwuemeka et al., 2018, 2020; Verdecchia et al., in revision]. Our seismicity relocation illustrates a diffuse distribution around the rift faults within the impact structure, in contrast to the outside where clusters are subparallel to the St. Lawrence River. Earthquake corner frequency fits using spectral ratios found stress drop values range between 2-200 MPa for events of M_w 2-4, typical of intraplate earthquakes. Events within the impact structure have higher average stress drop values relative to those outside. These source property differences may indicate the presence of a distributed fracture network and compositional alteration within the impact structure, which is corroborated by our 3D crustal velocity structure imaging and rock mechanical property analysis. Finally, we performed moment tensor inversion of 161 events (2000-2018) and combined with 64 additional solutions (1974-1997) from previous studies. This rich FMS dataset allowed us to invert stress field for the CSZ, which reveals a systematic ~60° clockwise rotation of the maximum horizontal stress, SHmax, with depth from the NE-SW orientation (borehole breakouts) to NW-SE approaching the Glacial Isostatic Adjustment estimated maximum strain direction. In summary, our studies highlight the importance of evaluating regional geological inheritance and local stress perturbation in order to adequately understand earthquake mechanisms and estimate the seismic hazard in an intraplate discrete seismic zone such as CSZ.

O 25. Tsunami modeling of a new seismic source on the north shore of Cuba

Stephen R. McNutt (University of South Florida, smcnutt@usf.edu) and E. Suleimani (University of Alaska Fairbanks)

On January 9, 2014 a M=5.1 earthquake occurred on the north shore of Cuba. The event was dip-slip on a steeply dipping fault, oriented approximately WNW-ESE. The location is the site of offshore islands, also oriented WNW-ESE, with a total length of about 200 km. This suggests that larger seismic events are possible on these structures. The earthquakes are only 90 miles from the south shore of Florida. We modeled potential tsunamis from a fault oriented WNW-ESE and dipping at 90 degrees. To represent shaking from a M=7.5 earthquake we used a length of 95 km, a width off 10 km, and slip of 1 m. The modeling was performed using a numerical model (Nicolsky et al., 2011) and was run at the UAFGI. Results show small heights of 3-8 cm at Key West, Everglades National Park (ENP), Marco Island and Miami. Maximum heights of 0.4 m are observed

near the source. Travel times for initial wave are: ENP 15 min; Key West 28 min; Miami 30 min; Marco Island 240 min. The peak wave occurs 10 to 50 min later and varies by location We also modeled slip with reversed polarity because some aftershocks of the January 2014 earthquake showed reverse slip – the models gave the same heights and times but reversed polarity. This is likely because the grid for bathymetry is coarse (3x3.7 km pixel size) so detailed interaction with the shore is not well represented. We modeled a larger event by increasing the slip while holding other parameters constant. This resulted in a M7.8 hypothetical event, with higher amplitudes but similar time histories. These results suggest that South Florida would experience only a modest hazard from tsunamis generated by earthquakes on the north shore of Cuba. This could change if submarine landslides or other interactions occurred.

P 26. Void detection using distributed acoustic sensing ambient noise interferometry
M. Mirzanejad (Tetra Tech), D. O'Connell (Tetra Tech), M. Isaacson (Tetra Tech), **Will Levandowski** (Tetra Tech), and J. Nuttall (Tetra Tech)

Sinkhole formation due to the collapse of sediments into subsurface voids is problematic in many industries. Every year, millions of dollars' worth of damage are caused by failure to identify near-surface voids in various projects. Particularly in active karst-forming environments, sinkholes may form after the project operations have started and can lead to catastrophic failures causing irreparable damage to the property and surrounding environment. Invasive testing techniques require that a probe physically intersect the underlying potential voids for successful detection. Nondestructive techniques provide a complementary option for subsurface void detection over a large volume of the underlying material. Seismic methods are particularly well suited for shallow and deep void detection in various environments. Active seismic source testing using an array of nodes or geophones on the ground surface has been the method of choice for void detection applications. Nonetheless, the prolonged deployment of nodal and geophone arrays may not be feasible in specific mining applications or harsh environments. Furthermore, active testing methods have limitations since not all surface conditions can accommodate the deployment of a large source for seismic acquisition surveys. Distributed acoustic sensing (DAS) as an emerging technology does not have many limitations of traditional arrays and can easily be deployed to measure ambient noise fluctuations. This study analyzes the feasibility of using such a method for void detection and subsurface material characterization. Numerical experiments are performed by placing a DAS array on the surface for various array geometries and channel spacings. Ambient noise emissions are synthetically modeled and are recorded by the DAS array. Different seismic imaging techniques are then employed for subsurface characterization and void detection. A relationship between array size and geometry, channel spacing, void size, and depth is established and reported using various seismic imaging techniques. The findings of this study provide insight into the application of DAS using ambient noise interferometry for void detection in future field-testing applications.

***P 27. Near-surface P-wave velocity near West Miami, Florida from quarry blast records**
Elham Moslemi (elhammoslemi@usf.), S. McNutt, G. Thompson, and J. Braunmiller (all University of South Florida)

We used blast records from several limestone quarries in the Miami Lakes area (25.6°N, -80.3°W) northwest of Miami, Florida to estimate shallow P-wave velocities. Prior knowledge of the velocity model was lacking. We deployed a network of ten Raspberry Shake seismometers (six 3-component, four 1-component with co-located infrasound) at residential homes in the Miami Lakes region and visually identified 1422 blasts from July 2019 to May 2022. We manually picked 1450 P-phase and air-wave arrivals using the earthquake analysis software SEISAN. We know the exact locations of 350 blasts (November 2021 to June 2022) from the Miami-Dade Pilot Program report and used a subset of 200 blasts with small location uncertainties in our catalog (average difference estimate-to-true: 0.9 km). The blasts occurred in three quarry areas known as White Rock Quarry (WRQ), Cemex, and Titan. We obtained average P-wave velocities from the quarries to the seismic stations of 4.36 to 4.56 km/s via linear regression. Blasts at WRQ that were nearest to the network (2 to 7 km)

allow precise picking and result in a well-constrained velocity of 4.36 km/s (R-squared 0.9). Blasts at the Cemex quarries occurred between 1 to 12 km distance and we obtained a velocity of 4.56 km/s. Blasts at the Titan quarries, 8 to 15 km from the network, result in an average near-surface P-wave velocity of 4.45 km/s. The velocities are consistent with expectations for the Pleistocene Miami Limestone that is extracted, and the small variations suggest relatively homogeneous material properties.

***O 28. Using a high-resolution earthquake catalog to unravel the M_w5.1 Sparta, North Carolina, earthquake sequence**

Miguel Neves (Georgia Tech, mjneves@gatech.edu), L. Chuang (Georgia Tech), W. Li (USTC), Z. Peng (Georgia Tech), and S. Ni (CAS)

On August 9, 2020, a M_w5.1 earthquake ruptured the uppermost crust near the town of Sparta, North Carolina. The earthquake ruptured a 2-km-long surface, likely the first surface-rupturing event in the Eastern United States since the New Madrid earthquake sequence (Figueiredo et al., 2022). Here we apply state-of-the-art earthquake detection and relocation techniques to better understand the local fault structures and the source processes of this and other intraplate earthquakes. Using a deep learning earthquake phase picker (EQTransformer, Mousavi et al., 2020) together with matched filter detection, we improve the earthquake catalog for the sequence. We detect a total of 7001 events for the period of August 1 to November 18, 2020. Using cross-correlation derived differential-travel times we relocate 1762 earthquakes. Our relocated catalog shows two major lineaments that appear to illuminate two fault branches with a slight kink. These lineaments are consistent with our focal mechanism solution using the generalized cut-and-paste (gCAP) method that shows a thrust event with some strike-slip component and a moment magnitude of 5.13 with optimal centroid depth of 1.3 km. In addition, non-DC components of about 12%, implying the mainshock may have ruptured along complex fault geometries. One of our identified lineaments is consistent with surface observations of thrust faulting by Figueiredo et al. (2022) and the dip of our preferred nodal plane. First motion polarities of all events M>1.5 suggest mostly strike-slip focal mechanisms, including the mainshock. Our results suggest that the mainshock rupture occurred primarily along a thrust fault but initiated in a secondary blind strike-slip fault. These observations have potential implications on seismic hazard estimation in intraplate settings.

***P 29. High resolution site response to Northern Oklahoma using dense Nodal array and its relationship to the shallow subsurface.**

Raymond Ng (University of Oklahoma, raymond.ng@ou.edu), X. Chen (Texas A&M), N. Nakata (MIT), and D. Dangwal (University of Oklahoma)

Earthquake hazard is an increasing concern as society continues to expand towards densely populated large cities built over basins. Increased seismicity and strong ground motion in Oklahoma with events larger than M5 within the last decade has led to an influx in earthquake hazard interest. To improve on understanding of ground motion amplification and characterize potential earthquake hazard, we conduct a site response study on a high density temporary linear nodal array near the city of Enid in Northern Oklahoma, using horizontal to vertical spectral ratio (HVSR) approach on ambient noise. Traditional site response investigations use historical data and other seismic sources such as earthquakes, vibroseis, and explosives. However, low aperture, cost, and infrequent major events cannot produce a dense high spatial coverage resolution. We remedy this by monitoring a 22km section of highway 412 east of Enid using 39 nodal sensors, which were co-located with a distributed acoustic sensing array using dark fiber and an interrogator. During our survey, we observe significant anthropogenic noise sources such as traffic, trains, and city noise, which are contained in frequencies (>1.5Hz) as well as low frequency secondary microseism (<1.5Hz). Small local events (Ml 2.3) within 10km epicentral distance were also recorded. High frequency dispersive surface waves within 1.5 – 4Hz are used to invert for shear velocity structure up to ~600m depth. We compare our site amplification profile derived from nodal-fiber data with Vs30 model and observe strong correlation between the fundamental frequency of ambient noise HVSR ratio and shallow (<100 m) shear velocity model. Using recorded local

earthquakes, we find significant low frequency amplification that differs from ambient noise HVSR, suggesting deeper basement structure influences seismic ground motion. Our results highlight the capability of passive seismic methods for high resolution Vs imaging, which can be used to for improving seismic risk assessment.

O 30. An initial examination on annual variations of seismicity at two intraplate regions

Zhigang Peng (Georgia Tech, zpeng@gatech.edu), Yanyan Zhang (Southern Univ. Sci. Tech.), Lingling Ye (Southern Univ. Sci. Tech.), Phuc Mach (Georgia Tech), and Miguel Neves (Georgia Tech)

Several recent studies have shown that annual variations of surface processes (e.g., atmospheric pressures, ocean loading, and groundwater storages) are capable of modulating seismic activities along major plate boundaries. However, it is still unclear whether such patterns are also present in intraplate regions, where the background seismicity rate is generally a few orders of magnitude lower. On the other hand, when the tectonic loading and seismicity rates are relatively low, we would expect to see a more pronounced effect in the annual variations of the seismicity rate, if they exist. Here we examine several intraplate regions with different space-time windows and magnitude thresholds to better quantify such temporal patterns. These include multiple historic earthquake catalogs along the North-South Seismic Belt in Southwest China, and a recently built high-resolution earthquake catalog along the Eastern Tennessee Seismic Zone (ETSZ) in the Southeastern United States. In each case, we use several de-clustering techniques such as the epidemic type aftershock sequence (ETAS) model or the nearest neighbor method to remove dependent events, and then group them based on the known focal mechanisms. Our preliminary results suggest that large strike-slip earthquakes in Southwest China primarily occurred in the late summer months (including the M_w 6.6 Luding earthquake on September 5, 2022, along the Xianshuihe fault), while thrust-faulting earthquakes such as the 2008 M_w7.9 Wenchuan earthquake tended to occur in April and May right before the Monsoon season. In the ETSZ, there is a preference for more earthquakes to occur during the time window when the groundwater levels (including reservoir water heights) change are the largest. Our next step is to evaluate their statistical significance and compare them with other regions to better understand the possible link between surface processes and earthquake activities in the intraplate regions.

***O 31. Site characterization in New England using high resolution geology maps and a subregion grouping layer**

Marshall A. Pontrelli (Tufts University, Marshall.Pontrelli@tufts.edu), L. G. Baise (Tufts University), and J. E. Ebel (Boston College)

To perform seismic risk analysis at any scale, knowledge of soil characteristics is essential to estimate site response. In this research, we develop sets of site characterization maps for New England, a glaciated region with a high impedance contrast and few Vs30 measurements in the national dataset. We compile state scale surficial geologic maps and group f0 values from HVSR measurements by their respective surficial geologic units to develop distributions of f0 within each surficial geology. We then divide New England into 6 subregions using a digital elevation model and a methodology where we select pixels below an elevation threshold in each general subregion area. With this additional mapping layer, we develop f0 distributions of each geologic unit within each subregion independently of other subregions. We then compile shear wave velocity data to estimate the average overburden velocity (Vsavg) of the surficial geologic units in New England. Using the common relationship f0 = Vs/4d, we compute estimates for a range of depths within each unit polygon in all the subregions and then, using the layer-over-halfspace model, estimate distributions of Vs30 values across the New England region. We observe that Cape Cod and Long Island (the Atlantic Coastal Plain subregion) has consistently low f0 values (with an f0 median of 1 Hz) indicating deep sediments. We also observe that the glaciomarine clays of the Boston Basin (median 2.01 Hz) and the Coast of Lake Champlain (median 1.64 Hz) and the Glaciolacustrine clays of the Connecticut river valley (median 2.03 Hz) are the next lowest frequency units in the regional map. We discuss the attributes of the distribution of each main unit and compare across units, contextualizing the site characterization of each subregion within larger New England.

O 32. New crustal velocity models and earthquake relocations for the New Madrid Seismic Zone
Christine A. Powell (capowell@memphis.edu), C. A. Langston, and M.M. Withers (all University of Memphis)

Detailed P- and S-wave velocity (Vp and Vs) models and earthquake relocations are determined for the New Madrid seismic zone (NMSZ) based on local earthquake arrival time data in the CERI NMSZ catalog for the period 1997 to 2020. The dataset consists of 4,037 earthquakes, 61,880 P phases and 43,988 S phases. The total number of recording stations is 59. The velocity models provide much greater resolution along the major arms of seismicity than previous models and indicate the strong influence that the Reelfoot axial intrusion has on Reelfoot fault (RF) seismicity. Northern RF earthquakes in the depth range 4.65 – 6.65 km occur along the steep northeastern edge of the intrusion and deeper earthquakes occur within the intrusion, in a high Vp/Vs ratio region indicative of high pore pressure. The southern RF occurs in a low susceptibility portion of the intrusion marked by negative Vp and Vs anomalies, again suggesting the presence of elevated pore pressure. An exception is a gap in seismic activity below 6.65 km associated with Ridgely ridge. The gap is characterized by a low Vp/Vs ratio produced by a negative Vp anomaly but no Vs anomaly, suggesting the presence of an elevated block of granite rhyolite basement. The Ridgley fault crosscuts the foot wall of the southern RF. The presence of the Axial fault is indicated by a concentrated, linear band of seismicity extending to depths exceeding 10 km when the earthquakes are in highly fractured, very low Vp and high Vs granite rhyolite crust. Near the intersection of the RF, the Axial fault enters the Reelfoot intrusion, and the earthquakes become scattered and only extend to 6 km depth. The Bootheel lineament is imaged as a distinct band of negative Vp anomalies in the depth range 6.65 to 8.65 km.

***P 33. Fundamental site resonance frequencies in the Upper Mississippi Embayment from ambient noise HVSR using 5 Hz Nodal geophones**
Russel Rogers (University of Kentucky, rcro234@uky.edu), S. Carpenter (Kentucky Geological Survey), and Z. Wang (Kentucky Geological Survey)

Horizontal-to-vertical spectral ratio (HVSR) has often been used to estimate fundamental site resonance frequency (f0) using the recordings of broadband seismometers. In this study, the efficacy of using 5 Hz nodal geophones to estimate the fundamental resonance frequencies in the thick upper Mississippi Embayment sediments from ambient noise HVSR was evaluated. In Summer 2022, 30 nodes were deployed throughout the Jackson Purchase region of Kentucky for a minimum of 24 hours at locations where shear-wave velocity profiles had previously been obtained via seismic reflection and refraction. HVSR processing consisted of the following steps: 1) multiple 100 s windows that excluded transient signal were selected using anti-triggering; 2) amplitude spectra were calculated for the three orthogonal components for each window and smoothed using a Hann window; 3) smoothed horizontal amplitude spectra were combined and divided by the smoothed vertical-component amplitude spectra to form HVSR curves for each window; and 4) the frequencies of the lowest peaks on the mean HVSR curves were selected as f0 for most sites. Selecting the peaks corresponding to the fundamental resonance at some sites involved simultaneously interpreting HVSRs determined for nearby sites. Clear f0 peaks were observed at all but seven sites with frequencies ranging from 0.3 to 1.8 Hz. Theoretical f0 was also derived from 1-D linear site response model using shear-wave velocity profiles over bedrock half-spaces. Results demonstrate that theoretical f0 is comparable to the empirical f0 at most sites. In some cases, these clear empirical peaks differed significantly from theoretical ones, suggesting either that some published velocity structures may need reassessment or that 1-D modeling is inappropriate at those sites. Our results indicate that nodal geophones are capable of recording ground motions at sufficiently low frequencies to measure the fundamental site resonance frequency in the Upper Embayment

P 34. Classifying seismic events located in the North Central and Northeastern United States by EarthScope's Array Network Facility using Machine Learning

Jonathan Schmidt (jpsc230@uky.edu), N. S. Carpenter, and Z. Wang (all Kentucky Geological Survey, University of Kentucky)

EarthScope's Array Network Facility (ANF) detected and located local and regional seismic events during the operation of the Transportable Array (TA). Because of the TA's uniform (~70 km) station spacing and the approximate two-year station lifespans, the ANF database presents an important dataset for characterizing seismicity in the U.S., particularly in poorly monitored regions. However, because the ANF did not classify events as blasts or earthquakes, it is unknown how many unique earthquakes are in their database. In this study, we focused on the north central and northeastern U.S., where the ANF located 6,643 seismic events from 2010 through late 2015. We leveraged a Machine Learning (ML) based seismic waveform classifier which calculates the probability that the waveforms were produced by a mine or quarry blast or an earthquake. We obtained TA recordings from IRIS and used a short-time-average over long-time-average algorithm for quality control prior to ML processing. Through tests on a subset of 502 events that spanned the area of interest, we determined that using classification probabilities from four or more stations with standard deviations of those probabilities less than 0.39 permitted accurate events classifications for mean earthquake probability > 0.7 for earthquakes or < 0.5 for blasts. Events failing these criteria were manually classified. Using these parameters, only 929 (~14%) of those events required manual review, saving considerable analyst effort. Our results indicate that the vast majority of the ANF database for the north central and northeastern U.S. consists of blasts with only 61 (0.01%) of the events being earthquakes not located by other agencies.

***O 35. Shear-wave velocity profiles for obtaining amplification factors for reference site to local site conditions in the Blue Ridge and Piedmont provinces of South Carolina**

Ali Sedaghat (Clemson University, asedagh@clemson.edu), R. Andrus (Clemson University), C. Amevorku (Clemson University), I. Wong (Lettis Consultants International), G. Rix (Geosyntec Consultants), C. Carlson (Geosyntec Consultants), N. Ravichandran (Clemson University), V. S. Jella (Clemson University), and N. Harman (South Carolina Dept. of Transportation)

New South Carolina seismic ground motion hazard maps have been developed for reference site conditions as part of an ongoing study to develop probabilistic seismic hazard maps for the South Carolina Department of Transportation (Wong et al. 2022). The reference site conditions in the South Carolina Blue Ridge and Piedmont (SCBRP) provinces are characterized by median time-averaged shear-wave velocity in the top 30 m (Vs30) of 1,183 to 1,518 m/s, depending on general rock type (Andrus 2022). This study presents the base case shear-wave velocity (Vs) profiles to calculate amplification factors for reference site to local site conditions in the SCBRP through site response analyses. A total of 42 measured Vs profiles are compiled from various project reports and used to model the residual soil and saprolite that overlie the reference site conditions of partially weathered rock. The resulting median local site Vs profile ranges from 253 m/s near the ground surface to 402 m/s at a depth of 30 m. The transitions from reference to local site conditions are also modeled. Three sets of base case Vs profiles (i.e., median, lower range, and upper range) with varying depth to partially weathered rock are proposed to capture the epistemic uncertainty in Vs.

***P 36. Seismic anisotropy beneath the Eastern North American Margin from frequency-dependent shear wave splitting analyses**

Rajani Shrestha (University of Delaware, rajani@udel.edu) and C. Lynner (University of Delaware)

The rifting of the supercontinent Pangaea around 200 million years ago opened the Atlantic Ocean and deformed the lithosphere beneath the eastern margin of North America. This deformation is associated with an anisotropic fabric which seismic tools can observe at present. As anisotropy from current mantle flow in the asthenosphere also resides beneath the margin, further constraints on the anisotropic signals from the

lithosphere and the asthenosphere is necessary to further our understanding of how continents break apart and how the mantle flows beneath passive margins. We present shear wave splitting measurements for teleseismic shear waves recorded at seismic stations (EarthScope Transportable Array and US national network) from Georgia to Virginia in the eastern US in three different frequency ranges: low (10 – 50 s), mid (5 – 10 s), and high (1 – 5 s) to investigate the anisotropic contributions from the two different sources. Our results show evidence of frequency dependence with almost all nulls in the low, abundant splitting in the mid, and mostly splits in the high frequencies. Even though there are few splits in the low, the average delay times decrease from the lower to the higher frequencies. The fast polarization directions vary from more E-W or NE-SW towards the continent to ~NNE-SSW (margin-parallel) near the coast, in general. The change in splitting pattern between the three frequencies indicate the presence of layered anisotropy beneath the region, which we model using splitting measurements from long-run US network stations having >10 years of data.

P 37. Accelerated coastal erosion at Kennedy Space Center: how do seismo-acoustic waves from rocket launches affect groundwater movement?

Glenn Thompson (University of South Florida, thompsong@usf.edu), S. Krupa, K. Locher, and K. Blair

Rapid beach erosion (4-7 m per year) along the coast at Kennedy Space Center (KSC) is faster than in adjacent areas, potentially threatening billions of dollars of infrastructure. We explore whether groundwater movement from rocket launches is a significant contributor to this erosion. If so, the increased frequency and thrust of rockets could accelerate erosion further. In March 2022, we installed Campbell Scientific piezoelectric pressure transducers, temperature sensors, and atmospheric pressure sensors in two wells (depths 4.6 and 9.1 m) with an above-ground barometer about 500-m SSE of launch complex 39A to continuously monitor groundwater at a sampling frequency of 100 Hz. USF deployed a co-located seismo-acoustic station. Data from the May 18th launch of a Falcon 9 rocket suggest that water level changes are caused by ground-coupled infrasound waves, rather than direct seismic waves. However, piezoelectric sensors appeared to record "ringing", overestimating water level changes. In July 2022, that equipment was removed and replaced by vibrating wire sensors, again sampled at 100 Hz. As a cross-check, water tubes were deployed in each well. These passive devices record only the maximum water level change. During the July 24th launch of a Falcon 9 rocket we recorded maximum displacement in the water tubes located in the shallow and intermediate wells of 6.95 cm and 10.3 cm respectively, compared to 7.74 cm and 8.43 cm for vibrating wire sensors. We have much more data to analyze, but our preliminary hypothesis is that as the ascending rocket generates infrasound jet noise, this energy couples into the ground over a broad region causing rapid oscillations in pore pressure, which squeezes out groundwater. While the infrasound energy dissipates within ~1 minute, this wave of expelled groundwater then likely flows towards the coast over a longer timescale, accelerating erosion.

P 38. A pipeline for near-real-time seismo-acoustic monitoring of quarry blasts in the Miami Lakes region

Glenn Thompson (thompsong@usf.edu), J. Braunmiller, S. McNutt, F. Rodriguez Cardozo, M. Hastings, and E. Moslemi (all University of South Florida)

The best construction limestone in Florida is mined at several quarries in Miami Lakes area (25.6°N, -80.3°W), northwest of Miami. As more residential communities are built close to these quarries, homeowner complaints about blasting have increased. Since July 2019, USF Geosciences has visually identified 1422 blasts as part of a Masters project (Moslemi et al., this conference). The Florida government is interested in understanding why these blast events are so strongly felt by the local community, and an essential step is to create a high quality catalog of these events and instrumental measurements of the ground motion they cause. Our project aims to meet this goal and demonstrate an operational capability to detect, classify, locate and quantify these blast signals, using Raspberry Shake instruments already deployed in the area. Real-time data acquisition can be readily accomplished using Earthworm, Antelope, or SeisComP3. For our proof-of-concept, we have instead built a near-real-time system. On a daily cronjob, our pipeline automatically downloads Raspberry Shake data, writes it to an SDS archive, encapsulates it within an Antelope waveform database, plots web-based

spectrograms, detects, locates, and estimates the magnitude of each event. Additional database tables are populated with amplitude (e.g. PGA, PGV, PGD), energy, and frequency metrics computed on each seismic and infrasound channel. All these derived data are summarized on various plots and reports available on a website. Finally, events are manually reviewed and classified, with phase picks added, modified, or deleted as necessary. Web-based plots and reports are updated accordingly. The analyst-reviewed catalog is also mirrored into a Seisan database to support the previously mentioned Masters project. Soon we intend to add a diagnostic monitoring system to track data outages and other data quality issues. Our pipeline is flexible, and can easily be used for non-Raspberry-Shake stations too.

P 39. Accuracy considerations in the implementation of deep-learning earthquake detection
Jacob I. Walter (University of Oklahoma, jwalter@ou.edu) and P. Ogwari (University of Oklahoma)

The proliferation of new and better machine-learning, and especially deep-learning pickers, in the scientific literature seems to be outpacing the implementation of them in operational networks and research workflows. Based on our experience in implementing deep-learning pickers, our experience suggests that deep learning pickers in production environments would not come without some tradeoffs in accuracy of the scientific product. Over the last few years, we have continued the development of easyQuake (https://github.com/jakewalter/easyQuake) that consists of a flexible set of tools for detecting and locating earthquakes from FDSN-collected or field-collected seismograms. We will show a comparison of several different deep learning pickers that are user-selected within easyQuake and show relative tradeoffs between different detection capabilities for case studies that include Oklahoma and Puerto Rico. We will explore the systematic bias evident down to the timing of phase pick arrivals relative to human-picked phase arrivals. In addition, we will discuss pitfalls that include how the selection of training data may affect the performance of the detection. These nuances have important considerations for research endeavors and real-time seismic networks considering expanding the use of machine-learning for earthquake detection.

***O 40. Quantifying seismic noise change in urban and rural regions in Québec, Canada**
Lan Xi Zhu (McGill University, lan.zhu@mail.mcgill.ca), Y. Liu (McGill University), and A. F. Peña Castro (University of New Mexico)

A broadband seismometer captures ground vibrations from various sources in addition to earthquakes. In fact, the recorded continuous waveforms reveal rich information about the ambient noise of the environment where the seismometer is located. Quantifying the characteristics of natural and anthropogenic seismic noises is therefore important for understanding the environment we live in. Here we analyze multiple-year (2015 - 2021) continuous seismic recordings in both urban and rural settings in Québec, eastern Canada, using SeismoRMS (Lecocq et al., 2020) that computes ground motion root mean squared (RMS) displacement vs. time. Three stations in major cities and five stations in remote areas along the coasts of the St. Lawrence River are selected to represent urban and rural environments, respectively. We mainly focus on the high-frequency (4.0 to 14.0 Hz) band where anthropogenic seismic noise dominates. Our preliminary results show consistent seasonal variation across all stations in both urban and rural regions, where warmer months are observed to be noisier because of increasing outdoor activities and construction projects. Periods of lower noise level due to shorter time scale events, such as New Year holiday seasons and the two-week Québec provincial construction holidays in July, are also observed in the seismic recordings. In 2020, we observe a reduction in urban high-frequency seismic noise in response to the COVID-19 global pandemic. Such an effect is less prominent in the less-populated rural regions. We also explore a lower frequency band (0.1 to 1.0 Hz) where natural sources, in particular ocean microseisms, become important. The observed seasonal variation with higher noise level in winter agrees with previous studies and is consistent throughout the study period at all eight stations. This study is the first to systematically quantify how human activities influence seismic data recordings in different regions in Québec.